



Published in final edited form as:

Opt Lett. 2009 April 1; 34(7): 953–955.

Scanning fiber-optic nonlinear endomicroscopy with miniature aspherical compound lens and multimode fiber collector

Yicong Wu^{1,2}, Jiefeng Xi^{1,2}, Michael J. Cobb¹, and Xingde Li^{1,2,*}

¹*Department of Bioengineering, University of Washington, Seattle, Washington 98195, USA*

²*Currently with Department of Biomedical Engineering, Johns Hopkins University, Baltimore, Maryland 21205, USA*

Abstract

A flexible scanning fiber-optic endomicroscope using a miniature compound lens and a multimode-fiber (MMF) collector was developed for two-photon fluorescence (TPF) and second-harmonic generation (SHG) imaging. The compound lens consisted of a pair of aspherical lenses and exhibited reduced chromatic aberration compared with gradient-index lenses, thus increasing the TPF/SHG collection efficiency. The introduction of a short MMF collector at the distal end of the double-clad fiber of the endomicroscope further mitigated the adverse influence of chromatic aberration of the lens and enhanced the TPF/SHG collection efficiency. Both ray-tracing simulations and experiments on TPF imaging of fluorescent beads and SHG imaging of rattail tendon demonstrated approximately nine (approximately four) times improved collection efficiency for TPF (SHG) with the new endomicroscope design that utilized a compound lens and an MMF collector.

Two-photon fluorescence (TPF) and second-harmonic generation (SHG) microscopy are powerful techniques for high-resolution imaging of biological tissues [1]. With the advances in micro-optics and micromechanical components, a TPF/SHG endomicroscopy system is becoming attractive as a basic research tool and has the potential for *in vivo* clinical applications [2,3]. Miniature objective lens is one of the key components in a TPF/SHG endomicroscope and ideally should be achromatic over a broad spectral range (e.g., from near-IR excitation to visible fluorescence or SHG signals). Gradient-index (GRIN) lenses, owing to their small diameter and cylindrical geometry, have been commonly used as the objective lens in an endomicroscope [2–6]; however, they suffer severe chromatic aberration, causing a considerable focal shift between the excitation (near-IR) and the TPF/SHG signals. For a compact, single-fiber excitation laser delivery and TPF/SHG collection configuration [e.g., with a single double-clad fiber (DCF)], chromatic aberration and the associated large focal shift will result in severe reduction in the TPF/SHG collection efficiency compared with a standard microscope system owing to the small collection area in the fiber.

In this paper, we report the use of a miniature compound lens to minimize the chromatic aberration and increase the TPF/SHG collection efficiency. In addition, a short piece of multimode fiber (MMF) was introduced at the distal end of the DCF (e.g., by thermal splicing) to mitigate the influence of chromatic aberration and further improve TPF/SHG collection. Ray-tracing analyses were conducted to investigate the improvement of TPF/SHG collection efficiency and to compare the performance of the compound lens with a GRIN lens.

Experiments were also carried out, and the results demonstrated that the new and easy-to-implement miniature compound lens and the MMF collector improved the TPF and SHG collection efficiencies by at least a factor of 9 and 4, respectively.

Figures 1(a)–1(c) respectively show the schematic, a photo of the distal end optics, and a photo of the assembled scanning endomicroscope equipped with a miniature compound lens and an MMF collector. The fiber-optic probe basically consisted of a DCF (Fibercore, Ltd.) with a short MMF fused at its end (where single-mode excitation laser was delivered through the core and multimode TPF/SHG signals were collected through the inner clad), a small tubular piezoelectric actuator (for resonantly sweeping the DCF tip for 2D beam scanning), and a miniature compound lens for beam focusing. The compound lens was made of a pair of 3 mm miniature aspherical lenses (modified from Archer OpTx L150 and L110 lenses), which had a usable diameter of 2.2 mm and were assembled with an ~ 1 mm separation to provide an overall magnification of 0.32 from the fiber tip to the sample and a measured working distance of 0.65 mm. A 300- μm -long MMF (105/125 μm core/clad and 0.22 NA) was spliced at the distal end of the DCF. The length (300 μm) of the MMF collector was chosen such that it would shorten the distance between its end surface and the back focus of the nonlinear optical signals as much as possible while not bending/distorting the excitation beam. Here, the MMF had almost the same core size and NA as the inner clad of the DCF, and its short length did not significantly influence the excitation beam path. As confirmed with ray-tracing simulations (and soon explained in detail), the short MMF collector guided more nonlinear optical signals back to the DCF.

To quantitatively understand the adverse effect of chromatic aberration in a TPF/SHG endomicroscope, ray-tracing analyses on the TPF/SHG collection efficiency were performed for the compound lens and compared with a GRIN lens of a 1.8 mm diameter. Both configurations had the same magnification of 0.32 from the fiber tip to the sample and the same NA of 0.5 on the sample side. Figure 2(a) shows the representative ray plots for excitation light (in the forward direction, i.e., from the DCF to the sample) and nonlinear optical signals (in the backward direction). As can be seen, the back focus of nonlinear optical signals from the excitation focal volume within the sample falls in front of the DCF tip owing to the lens chromatic aberration. Figure 2(b) quantitatively describes the chromatic longitudinal focal shift from the DCF tip at the nonlinear optical wavelengths with 810 nm excitation. It is found that the back focal points of nonlinear signals (405–500 nm) when using a GRIN lens are ~ 1.8 – 1.0 mm in front of the DCF tip, which will dramatically reduce the TPF/SHG collection efficiency. In comparison, the aspherical compound lens exhibits less chromatic aberration (e.g., with an ~ 1.0 – 0.5 mm chromatic longitudinal focal shift), resulting in a higher TPF/SHG collection efficiency. It is also noted that the addition of a short MMF collector at the DCF tip shortens the distance between the back focus of the nonlinear optical signals and the end surface of the guiding collector, thus further improving the TPF/SHG collection efficiency.

Figure 2(c) summarizes the collection efficiency of the nonlinear optical signal as a function of wavelength (through the core and inner clad of the DCF) calculated by ray tracing when using (1) the GRIN lens, (2) the compound lens without the MMF collector, and (3) the compound lens with the MMF collector, with 100% representing full collection of the backreflected TPF/SHG signals by a perfect achromatic lens. The excited TPF/SHG signals are assumed to be backreflected isotropically with an NA of 0.5. These quantitative analyses indicate that the compound lens increases the collection efficiency of the DCF over the GRIN lens by a factor ~ 4.6 and ~ 5.4 for the TPF (at 530 nm) and SHG (at 405 nm) signals, respectively. The analyses also show that the MMF collector spliced at the end of the DCF further improves the collection efficiency by another factor of ~ 2.8 for TPF and ~ 1.9 for SHG. Overall, the combination of the compound lens and the MMF collector increases the collection efficiency of TPF/SHG signals by a factor of ~ 10 – 13 over the GRIN lens configuration.

Experiments were conducted to quantitatively demonstrate the improvement on the collection efficiency by the new design. Two configurations were considered for the endomicroscope, i.e., a GRIN lens with a DCF (without a MMF collector) and a compound lens with a DCF plus a 300- μm -long MMF collector. An all-fiber-optic scanning endomicroscope was built for each configuration. The scanning mechanism was similar to the one in our previous endoscopes [4,7]. In essence, 2D beam scanning in an open–close spiral pattern was realized by a tubular piezoelectric actuator, which was driven by triangularly modulated sinusoidal waveforms at the resonant frequency of the fiber cantilever. Both endomicroscopes had a circular scanning frequency of ~ 1500 Hz, corresponding to an imaging speed of 3 frames/s with each frame consisting of 512 circular scans. A scanning area of 120 μm in diameter on the sample was achieved with a drive voltage of $\sim \pm 30$ V for both configurations. Excitation pulses of 60 fs from a home-built Ti:sapphire laser were negatively prechirped by a photonic bandgap fiber [(PBF) HC-800-02, Crystal Fibre A/S] to compensate the positive dispersion within the DCF core. A pulse width of less than 200 fs at the sample could be achieved even with 50 mW delivered through the DCF core when the length ratio of PBF to DCF was ~ 1.1 .

To quantitatively compare the collection efficiency of the endomicroscopes with the above two configurations, we conducted real-time TPF imaging of a monolayer of 4.86 μm fluorescein beads. Figures 3(a) and 3(b) show representative TPF images collected with the GRIN lens–DCF configuration, and the compound lens–DCF plus the MMF collector, respectively. The imaging conditions were kept the same for both configurations. The maximal fluorescence intensities, averaged over about 100 beads in 10 representative images for each configuration as shown in Figs. 3(a) and 3(b), are 1 ± 0.15 and 8.73 ± 1.12 a.u. (mean \pm standard deviation) for the two configurations, respectively. Overall, there was about 8.7 times enhancement with the compound lens and the MMF collector, and the experimental finding was close to the ray tracing prediction.

Figures 3(c) and 3(d) compare typical backward SHG images of formalin-fixed rattail tendon acquired by the two endomicroscopes. All the images were recorded from the tissue surface (roughly over the same area by best effort) and averaged for 10 frames. Fine tendon structures at the level of single collagen fiber bundle were clearly identified on both images, consistent with the fact that rattail tendon is dominant by Type I collagen, which is a bright SHG source [8]. The maximal SHG intensities averaged over the collagen fiber bundles indicated by the arrows in Figs. 3(c) and 3(d) are 1 ± 0.13 and 3.87 ± 0.46 a.u., respectively. For the brightest collagen fiber bundle as surrounded by the ellipse in each figure, the averaged SHG intensities in Figs. 3(c) and 3(d) are 1 ± 0.15 and 4.36 ± 0.74 a.u., respectively. Overall, quantitative analysis of the images indicated the endomicroscope with the compound lens and MMF collector increased the SHG collection efficiency by a factor of ~ 4 . The discrepancy of this improvement with the predicted ~ 10 times improvement might be partially due to the polarization dependence of SHG intensity of collagen fibers, since the excitation light through the endomicroscope was partially polarized. In addition, the detected SHG signals were dominated by multiply scattered light, while ray-tracing simulations were based on the assumption that the SHG photons were directly reflected back to the objective lens (i.e., via single scattering).

In conclusion, an effective method was developed for improving the optical performance of a fiber-optic TPF/SHG endomicroscope by using a miniature compound lens and an MMF collector. Both ray-tracing simulations and experiments on TPF imaging of fluorescent beads and SHG imaging of rattail tendon were conducted, and the results demonstrated an improved signal collection efficiency by a factor of ~ 9 and ~ 4 for TPF and SHG, respectively.

Acknowledgments

The authors gratefully acknowledge the technical assistance from Boyd Hunter and Jeff Magula and the grant support from the National Institutes of Health (NIH) (CA120480 and CA116442) and the National Science Foundation (NSF) (Career Award XDL).

References

1. Zipfel WR, Williams RM, Christie R, Nikitin AY, Hyman BT, Webb WW. Proc. Natl. Acad. Sci. U.S.A 2003;100:7075. [PubMed: 12756303]
2. Helmchen F, Fee MS, Tank DW, Denk W. Neuron 2001;31:903. [PubMed: 11580892]
3. Flusberg BA, Jung JC, Cocker ED, Anderson EP, Schnitzer MJ. Opt. Lett 2005;30:2272. [PubMed: 16190441]
4. Myaing MT, MacDonald DJ, Li XD. Opt. Lett 2006;31:1076. [PubMed: 16625908]
5. Fu L, Jain A, Xie H, Cranfield C, Gu M. Opt. Express 2006;14:1027. [PubMed: 19503423]
6. Fu L, Jain A, Cranfield C, Xie HK, Gu M. J. Biomed. Opt 2007;12:040501. [PubMed: 17867789]
7. Liu X, Cobb MJ, Chen Y, Kimmey MB, Li XD. Opt. Lett 2004;29:1763–1765. [PubMed: 15352362]
8. Campagnola PJ, Millard AC, Terasaki M, Hoppe PE, Malone CJ, Mohler WA. Biophys. J 2002;82:493. [PubMed: 11751336]

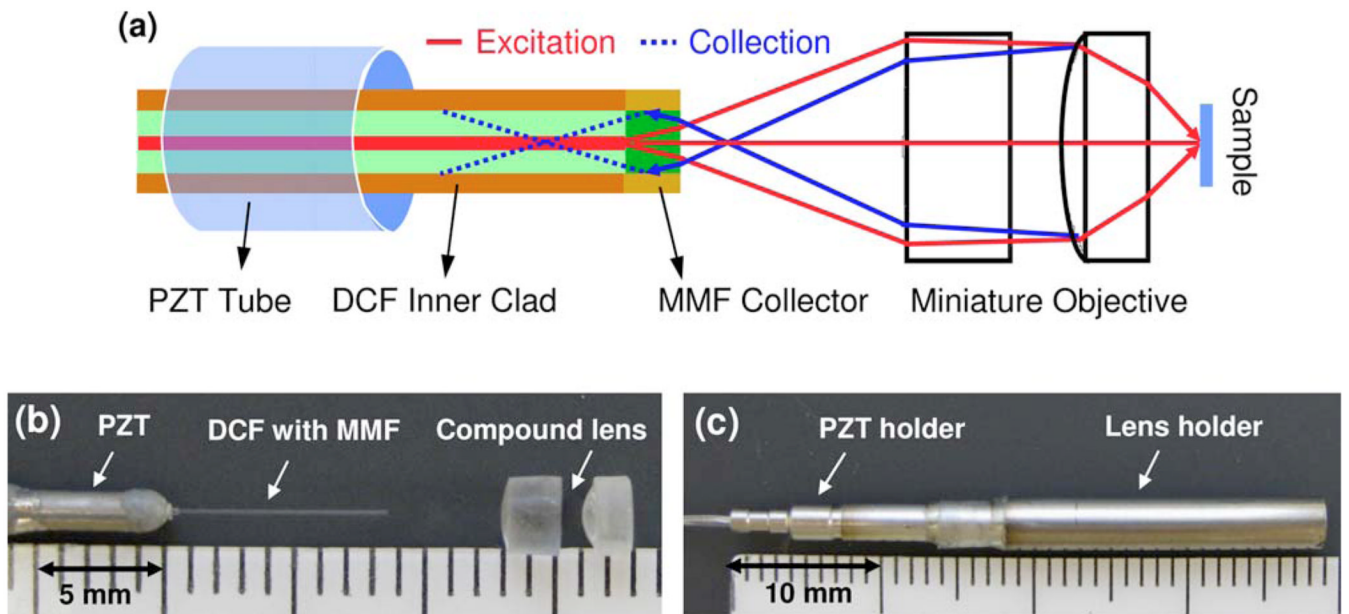


Fig. 1. (Color online) (a) Schematic of the fiber-optic scanning endomicroscope with a miniature aspherical compound lens and a multimode-fiber collector. (b) Photo of the distal end optics. (c) Photo of the assembled distal end of the endomicroscope with all the optical components and a piezoelectric transducer (PZT) resonant fiber scanner encased in a hypodermic tube.

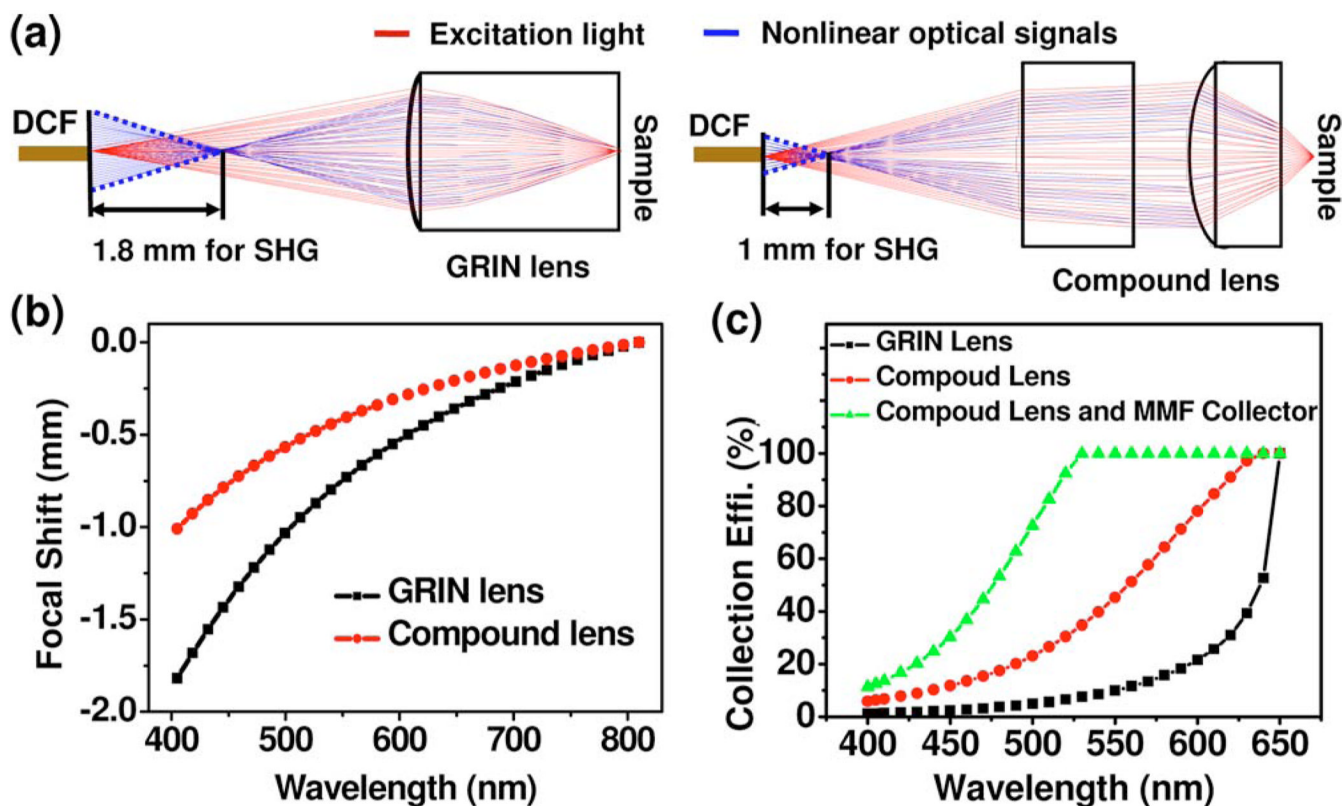


Fig. 2. (Color online) (a) Representative optical ray plots for excitation light and nonlinear optical signals when using the GRIN lens and the aspherical compound lens. (b) Chromatic longitudinal focal shift from the DCF tip for the nonlinear optical signals with 810 nm excitation when using the GRIN lens and aspherical compound lens. (c) Calculated collection efficiency of TPF/SHG signals when using the GRIN lens, the compound lens, and the compound lens plus the MMF collector.

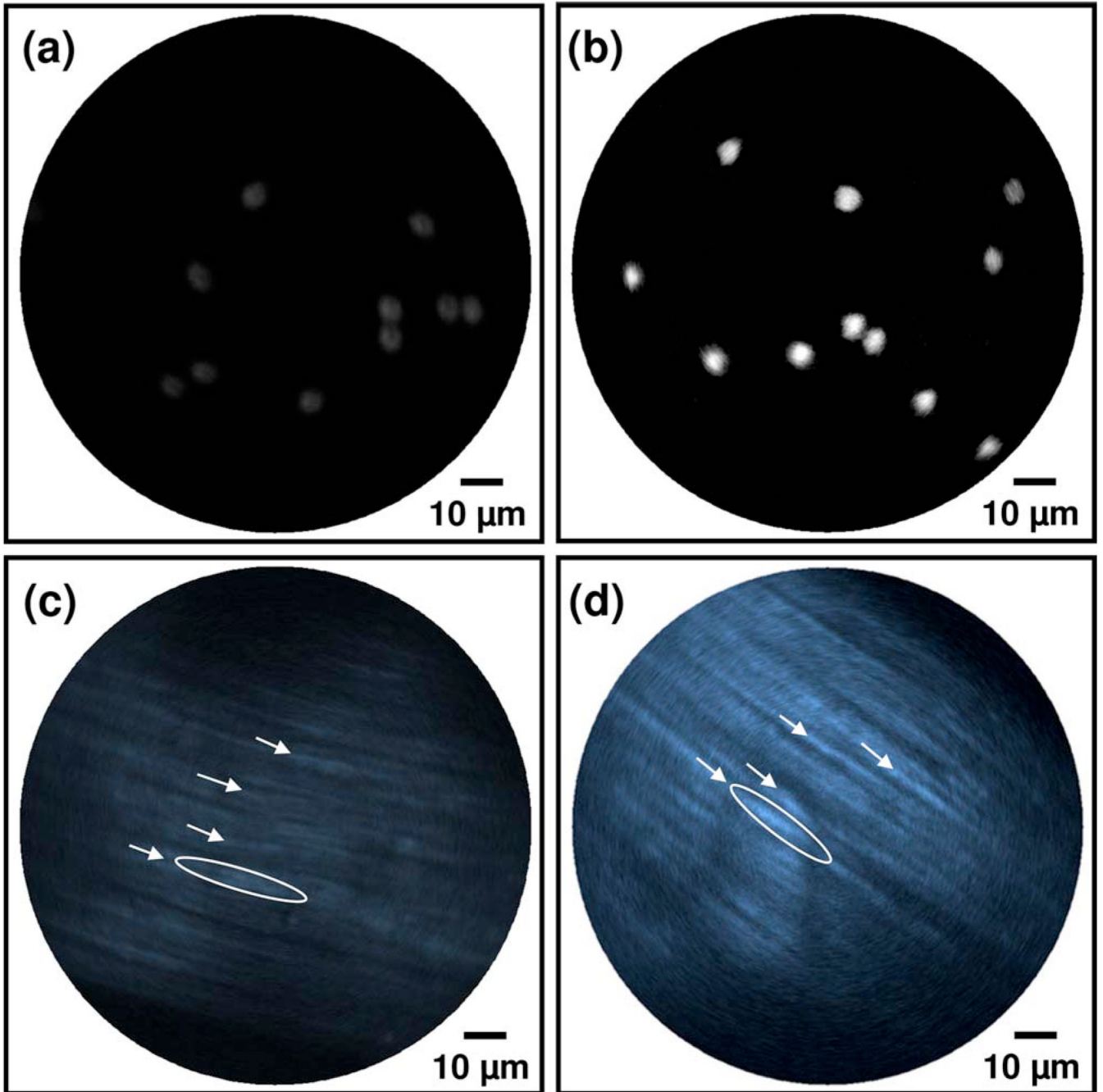


Fig. 3. (Color online) Typical TPF images of a monolayer of $4.86\ \mu\text{m}$ fluorescein beads [(a), (b)] and SHG images of formalin-fixed rattail tendon [(c), (d)] acquired by a scanning all-fiber-optic endomicroscope with the GRIN lens-DCF configuration [(a), (c)] and the compound lens-DCF plus the MMF collector [(b), (d)]. The averaged fluorescence intensity of the beads in (b) is about nine times as that in (a). The averaged SHG intensity of the fiber bundles indicated by the arrows or ellipses in (d) is about four times as that in (c). All the images were acquired under the same experimental conditions, and the images were shown without renormalization.